Rose-Hulman Institute of Technology

Rose-Hulman Scholar

Mathematical Sciences Technical Reports (MSTR)

Mathematics

7-24-2002

Fast Reconstruction of Cracks Using Boundary Measurements

Nicholas A. Trainor
Rose-Hulman Institute of Technology

Rachel M. Krieger

Follow this and additional works at: https://scholar.rose-hulman.edu/math_mstr

Part of the Numerical Analysis and Computation Commons, and the Partial Differential Equations Commons

Fast Reconstruction of Cracks Using Boundary Measurements

Rachel M. Krieger and Nicholas A. Trainor
Advisor: Dr. Kurt Bryan

MS TR 02-14

July 24, 2002

Department of Mathematics
Rose-Hulman Institute of Technology
http://www.rose-hulman.edu/Class/ma/

FAX: (812) 877-8883   PHONE: (812) 877-8391

Fast Reconstruction of Cracks Using Boundary Measurements

Rachel M. Krieger and Nicholas A. Trainor
Advisor: Dr. Kurt Bryan

July 24, 2002

Abstract

This paper develops a fast algorithm for locating one or more perfectly insulating, pair-wise disjoint, linear cracks in a homogeneous two-dimensional electrical conductor, using boundary measurements.

Contents

List of Figures

1 Introduction

The ability to characterize the interior of an object without incurring harm on it is an invaluable tool in industry. Thus, simplifying available techniques of non-destructive imaging has practical industrial purposes. One such technique is impedance imaging, or steady-state thermal imaging. Bryan and Vogelius offer uniqueness results in the identification of n cracks inside of a two dimensional region in [1], which were improved by Alessandrini and Diaz Valenzuela in [2]. In [3], Andrieux and Ben Abda employed the reciprocity gap formula to identify a single, perfectly insulating crack, and recently Ogborne and Vellela generalized this method for completely characterizing a single linear crack which is not completely insulating in [4]. In this paper, we will offer an alternative method for characterizing the location and length of a single, completely insulating, linear crack. The ideas from this method will then be employed in an algorithm characterizing multiple, completely insulating cracks.

2 The Forward Problem

Let Ω be a bounded region in $\mathbb{R}^2$ with boundary $\partial\Omega$. The steady state temperature at any point (x, y) lying inside of Ω will be denoted by $u(x, y)$. After appropriate scaling, we assume that $u(x, y)$ obeys the steady state heat equation

$$\frac{\partial^2 u}{\partial x^2} + \frac{\partial^2 u}{\partial y^2} = 0 \tag{1}$$

in Ω. We also assume that a steady state heat flux, g, is applied the external boundary, so that on $\partial\Omega$,

$$\frac{\partial u}{\partial \mathbf{n}} = g \tag{2}$$

where $\mathbf{n}$ is a unit outward vector normal to $\partial\Omega$.

Now suppose that n linear, completely insulating, pairwise disjoint cracks lie inside of Ω. Let σ_i denote the ith crack, $\mathbf{p}_i$ the midpoint of σ_i, $|\sigma_i|$ the length of σ_i, and θ_i the angle between the line containing σ_i and the x-axis, where $\frac{-\pi}{2} < \theta_i \leq \frac{\pi}{2}$. In general we will work under the assumption that $|\sigma_i| \ll \min\{|\mathbf{x} - \mathbf{p}_i|; \mathbf{x} \in \partial\Omega\}$. If we denote the collection of n cracks by $\Sigma = \bigcup_{i=1}^{n} \sigma_i$, we then assume that (1) holds for all $(x, y) \in \Omega \ / \ \Sigma$. Since we have assumed that heat flow across each crack σ_i is blocked completely, we have

$$\frac{\partial u}{\partial \mathbf{n}_{\sigma_i}} = 0 \tag{3}$$

for all i, where $\mathbf{n}_{\sigma_i}$ is the unit vector normal to σ_i equal to $< -\sin(\theta_i), \cos(\theta_i) >$. Note that condition (3) is assumed to hold on both sides of σ_i.

3

We also add the normalization $\int_{\partial\Omega} u \, ds = 0$. These conditions ensure a unique solution to the conduction problem (1)-(3).

For all i we will denote one side of σ_i as the "+" side, the other as the "−" side, in such a way that the vector $\mathbf{n}_{\sigma_i}$ points from the minus to the plus side. The superscript "+" will be used to denote the limiting value of a quantity from the plus side of σ_i, while the superscript "−" denotes the limiting value from the minus side of σ_i.

The solution u to the forward problem will be smooth away from the cracks, but in general will have a jump discontinuity across each crack. We will denote the jump function in u across a crack by $[u] = u^+ - u^-$. Standard elliptic regularity theory shows that $[u]$ is continuous (indeed, smooth) along any given crack and tapers to zero at the crack endpoints, typically with square root singularities at the crack tips.

Given (1)-(3), the forward problem consists of knowing the location of all σ_i in Ω, and from this, recovering the steady state solution, i.e. the temperature $u(x, y)$ for $(x, y) \in \Omega$. However, in this paper, we are interested in examining the inverse problem. Given (1)-(3) and measurements of u on $\partial\Omega$ we wish to find the midpoint, $\mathbf{p_i}$, length, $L_i = |\sigma_i|$, and angle, θ_i, of each crack.

3   Locating a Single Crack

3.1   Algorithm

Suppose for a moment that there are no cracks inside of Ω. Let $\Gamma(x_1, x_2) = \frac{1}{4\pi} \ln(x_1^2 + x_2^2)$ denote the fundamental solution for the Laplacian in two dimensions. Then by Green's Third Identity, we have that

$$\frac{1}{2} u(\mathbf{x}) + \int_{\partial\Omega} u(\mathbf{y}) \frac{\partial \Gamma}{\partial \mathbf{n_y}}(\mathbf{y} - \mathbf{x}) ds_y \; - \; \int_{\partial\Omega} \Gamma(\mathbf{y} - \mathbf{x}) \frac{\partial u}{\partial \mathbf{n_y}}(\mathbf{y}) ds_y \; = 0. \tag{4}$$

We will denote the left hand side of (4) as $\alpha(\mathbf{x})$ (so for a function harmonic in Ω we have $\alpha \equiv 0$). Note that we can compute $\alpha(\mathbf{x})$ for any $\mathbf{x} \in \partial\Omega$, as both $\frac{\partial u}{\partial \mathbf{n}}$ and $u(\mathbf{y})$ where $\mathbf{y} \in \partial\Omega$ are known.

Now suppose there are n cracks inside of Ω. In this case $\alpha(x)$ is not identically zero, but rather an application of the divergence theorem shows that

$$\alpha(\mathbf{x}) \; = \; \sum_{i=1}^{n} \int_{\sigma_i} \frac{\partial \Gamma}{\partial \mathbf{n}_{\sigma,i}}(\mathbf{x} - \mathbf{y}) \, [u](\mathbf{y}) ds_y. \tag{5}$$

For the remainder of this section, we will assume $n = 1$ and neglect the subscript on σ. We parameterize σ as

$$\{(y_1, y_2) : y_1 = p_1 + t \cos(\theta), \; y2 = p_2 + t \sin(\theta) \mid \frac{-L}{2} \leq t \leq \frac{L}{2}\},$$

which allows us to find $\frac{\partial \Gamma}{\partial \mathbf{n}_\sigma}(\mathbf{x} - \mathbf{y})$ explicitly, as

$$
\begin{aligned}
\frac{\partial \Gamma}{\partial \mathbf{n_y}}(\mathbf{x} - \mathbf{y}) &= \frac{1}{2\pi} \frac{-\sin(\theta)(x_1 - p_1 - t\cos(\theta))}{(x_1 - p_1 - t\cos(\theta))^2 + (x_2 - p_2 - t\sin(\theta))^2} \\
&+ \frac{1}{2\pi} \frac{\cos(\theta)(x_2 - p_2 - t\sin(\theta))}{(x_1 - p_1 - t\cos(\theta))^2 + (x_2 - p_2 - t\sin(\theta))^2} \\
&= \frac{1}{2\pi} \frac{(\mathbf{x} - \mathbf{p}, \mathbf{n}_\sigma)}{(\mathbf{x} - \mathbf{p}, \mathbf{x} - \mathbf{p}) - 2t(\mathbf{x} - \mathbf{p}, \hat{\sigma}) + t^2}
\end{aligned}
\tag{6}
$$

where $\hat{\sigma} = <\cos(\theta), \sin(\theta)>$. Since $\mathbf{x} \in \partial\Omega$, the quantity $\frac{\partial \Gamma}{\partial \mathbf{n_y}}(\mathbf{x} - \mathbf{y})$ is well-defined for $t \in (-L/2, L/2)$, and vanishes identically in t precisely when $(\mathbf{x} - \mathbf{p}, \mathbf{n}_\sigma) = 0$, which occurs precisely when $\mathbf{x} - \mathbf{p}$ is perpendicular to $\mathbf{n}_\sigma$. As a result we find that the computable quantity $\alpha(\mathbf{x}) = 0$ if and only if $(\mathbf{x} - \mathbf{p}, \mathbf{n}_\sigma) = 0$, which also occurs precisely when $\mathbf{x} - \mathbf{p}$ is perpendicular to $\mathbf{n}_\sigma$. Therefore there exist at least two points, $\mathbf{x}_a$, $\mathbf{x}_b \in \partial\Omega$ such that $\alpha(\mathbf{x}_a) = \alpha(\mathbf{x}_b) = 0$, and it follows directly that σ is contained in the line from $\mathbf{x}_a$ to $\mathbf{x}_b$. We can thus easily recover the line on which the crack lies. See Figure 3.1 below.

We now show how to approximate the midpoint $\mathbf{p}$ of the crack. Expanding equation (6) into a series in t and employing the assumption that the length of the crack is much less the minimum of the set of distances from $\mathbf{p}$ to some $\mathbf{x} \in \partial\Omega$ allows us to make the simplifying assumption

$$
\frac{\partial \Gamma}{\partial \mathbf{n_y}} \approx \frac{1}{2\pi} \frac{(\mathbf{x} - \mathbf{p}, \mathbf{n}_\sigma)}{(\mathbf{x} - \mathbf{p}, \mathbf{x} - \mathbf{p})}
$$

Therefore, (5) can be closely approximated by

$$
\alpha(\mathbf{x}) \approx \frac{1}{2\pi} \frac{(\mathbf{x} - \mathbf{p}, \mathbf{n}_\sigma)}{(\mathbf{x} - \mathbf{p}, \mathbf{x} - \mathbf{p})} \int_\sigma [u](\mathbf{y}) \, ds_y = J \frac{(\mathbf{x} - \mathbf{p}, \mathbf{n}_\sigma)}{(\mathbf{x} - \mathbf{p}, \mathbf{x} - \mathbf{p})},
\tag{7}
$$

where we write $J = \frac{1}{2\pi} \int_\sigma [u](\mathbf{y}) \, ds_y$.

As shown in [5], J is "generically" non-zero. Note that

$$
\frac{\alpha(\mathbf{x})}{J} \approx \frac{(\mathbf{x} - \mathbf{p}, \mathbf{n}_\sigma)}{(\mathbf{x} - \mathbf{p}, \mathbf{x} - \mathbf{p})}
\tag{8}
$$

follows directly from (7) for any $\mathbf{x} \in \partial\Omega$. Now, when $\mathbf{x} - \mathbf{p}$ is parallel to $\mathbf{n}_\sigma$, $(\mathbf{x} - \mathbf{p}, \mathbf{n}_\sigma) = |\mathbf{x} - \mathbf{p}|$, in which case we have $\frac{(\mathbf{x} - \mathbf{p}, \mathbf{n}_\sigma)}{(\mathbf{x} - \mathbf{p}, \mathbf{x} - \mathbf{p})} = \frac{1}{|\mathbf{x} - \mathbf{p}|}$. See Figure 3.1 below. Note that this quantity is negated if $\mathbf{x} - \mathbf{p}$ is antiparallel to $\mathbf{n}_\sigma$.

Let $\mathbf{x}_1, \mathbf{x}_2 \in \partial\Omega$ such that the line $(\mathbf{x}_1, \mathbf{x}_2)$ is perpendicular to the line $(\mathbf{x}_a, \mathbf{x}_b)$, and suppose the vector $\mathbf{x}_1 - \mathbf{p}$ is parallel to $\mathbf{n}_\sigma$, which means that the vector $\mathbf{x}_2 - \mathbf{p}$ is antiparallel to $\mathbf{n}_\sigma$. Then by (8) and the triangle inequality we have that

$$
|\mathbf{x}_1 - \mathbf{x}_2| \le |\mathbf{x}_1 - \mathbf{p}| + |\mathbf{p} - \mathbf{x}_2| = \frac{J}{\alpha(\mathbf{x}_1)} + \frac{-J}{\alpha(\mathbf{x}_2)},
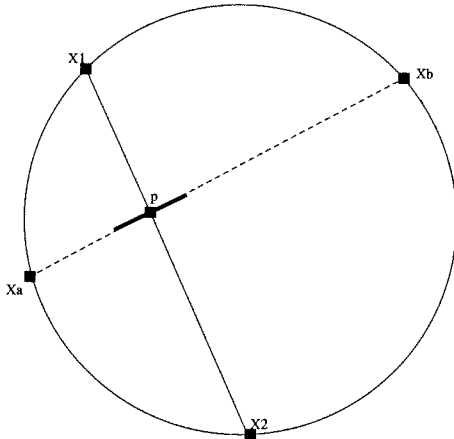\tag{9}
$$

5

Figure 1: Diagram for locating a single, perfectly insulating crack.

where equality holds only when $\mathbf{p} \in (\mathbf{x}_1, \mathbf{x}_2)$. Thus $\mathbf{p}$ can be approximated by taking pairs of points perpendicular to σ and selecting the specific pair, $(\mathbf{x}_1, \mathbf{x}_2)$, for which the equality in (9) holds. We thus recover $\mathbf{p}$ as

$$\mathbf{p} = (\mathbf{x}_1, \mathbf{x}_2) \cap (\mathbf{x}_a, \mathbf{x}_b).$$

Finally, we show how to recover the length of the crack, which is related to the jump integral $J = \frac{1}{2\pi} \int_\sigma [u](\mathbf{y}) ds_y$. As shown in [4] and [5], the quantity J is easy to compute, as follows. First, let $\psi(x, y) = -\sin(\theta)x + \cos(\theta)y$, where θ is the angle of the crack with the x-axis (which we have now determined). We then have

$$\int_\sigma [u](\mathbf{y}) ds_y = \int_{\partial\Omega} \left(u \frac{\partial \psi}{\partial \mathbf{n}} - \psi \frac{\partial u}{\partial \mathbf{n}} \right) ds \tag{10}$$

computable entirely from boundary data, and hence J is computable.

Finally, as shown in Section 5, we can approximate $J \approx \frac{\pi}{4} \nabla u_0 \cdot \mathbf{n}_\sigma L^2$, which means

$$L = \sqrt{\frac{J}{\frac{\pi}{4} \nabla u_0(\mathbf{p}) \cdot \mathbf{n}_\sigma}}. \tag{11}$$

Note that $\nabla u_0(\mathbf{p}) \cdot \mathbf{n}_\sigma$ is now known, and so L can be determined. Thus the entire crack—the midpoint $\mathbf{p}$, angle θ, and length L are determined.

3.2 Reconstruction Example

To provide a specific example of the algorithm used to locate a single, perfectly insulating crack, (and later examples of the numerical approximation of the location of multiple, perfectly insulating cracks), we take our domain Ω to be the unit disk in $\mathbb{R}^2$, and the flux on
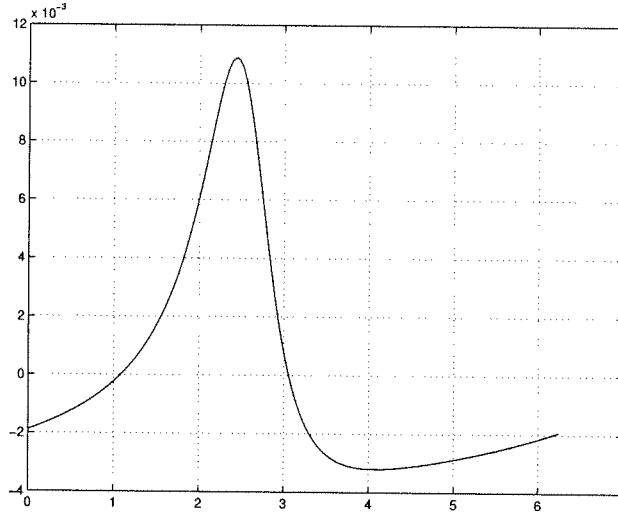
6

Figure 2: Graph of $\alpha(t)$ vs. t for boundary data generated by a single, linear, perfectly insulating crack inside of Ω.

$\partial\Omega$ to be $g = \sin(t)$, where Ω is parameterized as $(\cos(t), \sin(t))$ for $0 \le t < 2\pi$, and we can write $u(\mathbf{x}) = u(t)$ where $\mathbf{x} = (\cos(t), \sin(t))$. With this region and flux, we have that the harmonic solution over Ω is $u_0(x, y) = y$, $\nabla u_0 = <0, 1>$, $\int_{\partial\Omega} \frac{\partial \Gamma}{\partial \mathbf{n}}(\mathbf{x} - \mathbf{y})u(\mathbf{y})ds_y = 0$, and that $\int_\sigma \Gamma(\mathbf{x} - \mathbf{y})\frac{\partial u}{\partial \mathbf{n}}(\mathbf{y})ds_y = \frac{1}{2}\sin(t)$ for the point $\mathbf{x} = (\cos(t), \sin(t))$. Therefore

$$\alpha(\mathbf{x}) = \frac{1}{2}(u(t) - \sin(t)) \tag{12}$$

for $\mathbf{x} \in \partial\Omega$ and $0 \le t < 2\pi$.

In the example of locating both single and (later) multiple cracks, the boundary data, $u(\mathbf{x})$, for $\mathbf{x} \in \partial\Omega$ was generated by a C program using a boundary integral approach for solving the boundary value problem. In each example, data was generated for m equally spaced points about $\partial\Omega$. In each of the diagrams of the reconstructed cracks, the thick line segment represents the location of the actual crack, while the thin line segment represents the location of the estimated crack.

Using the method outlined in section 4, a single crack in Ω will be located. Therefore, we write all points $\mathbf{x} \in \partial\Omega$ for which we have temperature data as $(\cos(t), \sin(t))$, and determine $\alpha(t)$ for each of these points. Given data for m equally spaced points on the boundary, let $u(i)$ denote the temperature at the ith point on $\partial\Omega$, where $0 < i \le m$. By (12), $\alpha(\mathbf{x}) = \frac{1}{2}u(\cos(t), \sin(t)) - \frac{1}{2}\sin(t)$. Shown in Figure 3.2 is a graph of $\alpha(t)$ vs. t for some single, perfectly insulating crack inside of Ω.

We see that $\alpha(t_1) = \alpha(t_2) = 0$ where $t_1 \approx 1.0834353$ and $t_2 \approx 3.0582283$. Therefore, σ

7

lies on the line from

$$\mathbf{x}_a \quad = \quad (\cos(1.0834353), \sin(1.0834353)) \quad = \quad (0.4682958, 0.8835718)$$

to

$$\mathbf{x}_b \quad = \quad (\cos(3.0582283), \sin(3.0582283)) \quad = \quad (-0.9965272, 0.0832678).$$

We have thus identified the line on which σ lies. If desired, we can find θ by taking the arctan of the slope of the line from $\mathbf{x}_a$ to $\mathbf{x}_b$, and we find that $\theta = 0.5000355$ radians.

We can now use equation (10) to determine

$$
\begin{aligned}
\int_\sigma [u](\mathbf{y}) ds_y \quad &\approx \quad \sum_{k=1}^{m} u(i) \sin\left(\frac{2\pi(k-1)}{m} - \theta\right) \\
&\quad - \int_0^{2\pi} \sin(\phi)(-\sin(\theta)\cos(\phi) + \cos(\theta)\sin(\phi)) d\phi \\
&= \quad 0.027569154
\end{aligned}
$$

and so $J = \frac{\int_\sigma [u](\mathbf{y}) ds_y}{2\pi} \approx 0.0043878$.

We then take pairs of points on $\partial\Omega$ which define a line perpendicular to the line $(\mathbf{x}_a, \mathbf{x}_b)$. Using these pairs of points, we create a test function defined by

$$T(\mathbf{x}_1, \mathbf{x}_2) = \left(\frac{J}{\alpha(\mathbf{x}_1)} - \frac{J}{\alpha(\mathbf{x}_2)}\right) - |\mathbf{x}_1 - \mathbf{x}_2|$$

where the negative sign preceding $\frac{J}{\alpha(\mathbf{x}_2)}$ accounts for the negative value of $\alpha(\mathbf{x}_2)$ resulting from the fact that $\mathbf{x}_2 - \mathbf{p}$ is antiparallel to $\mathbf{n}_\sigma$. The pair of points, $\mathbf{x}_1$ and $\mathbf{x}_2$ resulting in a zero (and in fact, a minimum) of the test function define a line through the midpoint of σ. We find $\mathbf{x}_1 \approx (-0.7106844, 0.7040318)$ and $\mathbf{x}_2 \approx (0.2087861, -0.9779614)$. As $\mathbf{p} = (\mathbf{x}_1, \mathbf{x}_2) \cap (\mathbf{x}_a, \mathbf{x}_b)$ we find

$$\mathbf{p} \approx (-0.5148069, 0.3464550).$$

We have determined the midpoint and angle of the crack.

Finally, we know $\nabla u_0(\mathbf{p}) \cdot \mathbf{n}_\sigma = <0, 1> \cdot < -\sin(\theta), \cos(\theta) >= \cos(\theta)$. From equation (11) we find

$$L \approx \sqrt{\frac{8J}{\cos(\theta)}} \approx 0.1999967.$$

The true values used to general the boundary data were $\theta = 0.5$, $L = 0.2$ and $\mathbf{p} = (-0.512, 0.348)$. The reconstruction is diagramed in Figure 3.2, along with the lines $(\mathbf{x}_1, \mathbf{x}_2)$ and $(\mathbf{x}_a, \mathbf{x}_2)$, and the actual crack, σ_a, whose parameters are $\mathbf{p_a} = (-0.512, 0.348)$, $\theta_a = 0.50$ radians and $L_a = 0.20$ units. Note that the two cracks essentially coincide.
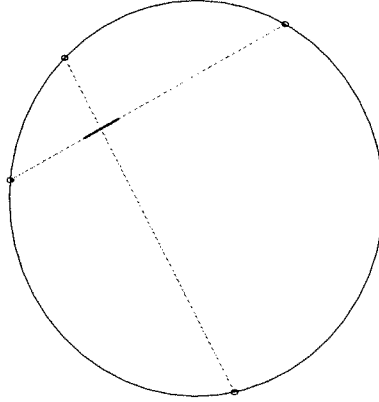
Figure 3: Reconstruction of a single crack via algorithm outlined in section 3.

3.3 Optimal Input Heat Influx

It is well-known that the input heat flux can have a dramatic effect on one's ability to detect and image a crack. In particular, if ∇u_0 is almost parallel to the crack then the crack is doing little to impede the flow of heat. Therefore, we would expect the perturbation of the boundary data caused by the crack, which is embodied in $\alpha(\mathbf{x})$, to be small and uninformative. This corresponds to the case in which the jump integral $J \approx 0$.

Throughout this section will we let $\mathbf{n}$ be the unit vector normal to the crack, and $\mathbf{m}$ be the unit vector normal to the boundary $\partial\Omega$, with $\mathbf{p}$ the midpoint of the linear crack. Thus in order to obtain the most information, we wish $\nabla u_0(\mathbf{p}) \cdot \mathbf{n}$ to be as large as possible. The direction and magnitude of $\nabla u_0(\mathbf{p})$ depends only on the Neumann data that we input, g. Thus we wish to maximize $\nabla u_0(\mathbf{p}) \cdot \mathbf{n}$ over all physically reasonable choices of g.

Let us first restrict ourselves to $g \in L^2(\partial\Omega)$. For a solution to

$$\triangle u_0 = 0 \text{ in } \Omega \tag{13}$$

$$\frac{\partial u_0}{\partial\mathbf{n}} = g \text{ on } \partial\Omega \tag{14}$$

to exist, we must have $\int_{\partial\Omega} g = 0$. Our goal is to find that choice for g which maximizes $\nabla u_0(\mathbf{p}) \cdot \mathbf{n}$. However it is clear that given a g, we can increase the magnitude of $\nabla u_0(\mathbf{p})$, and hence of the dot product, by simply multiplying g by any constant greater than 1. To exclude optimizing over this possibility we will impose the condition $\int_{\partial\Omega} g^2 \leq M$ for some $M > 0$.

For any point $(x_1, x_2) \in \Omega$, we can obtain the solution to (13)-(14) by

$$u_0(x_1, x_2) = \int_{\partial\Omega} N(x_1, x_2, y_1, y_2) g(y_1, y_2) \, ds_y \tag{15}$$

9

where N is the Neumann Kernel, which depends on the region Ω. Specifically, for any region $\Omega \subset \mathbb{R}^2$, the Neumann Kernel, N, for Ω is defined by

$$N(\mathbf{x}, \mathbf{y}) = \Gamma(\mathbf{x} - \mathbf{y}) + N_0(\mathbf{x}, \mathbf{y}) \tag{16}$$

for $\mathbf{x} = (x_1, x_2)$, $\mathbf{y} = (y_1, y_2)$, where N_0 is a function satisfying

$$\Delta_y N_0 = 0 \text{ in } \Omega \tag{17}$$

$$\frac{\partial N_0}{\partial \mathbf{m_y}} = -\left(\frac{\partial \Gamma}{\partial \mathbf{m_y}} + \frac{1}{|\partial \Omega|} \right) \text{ on } \partial \Omega \tag{18}$$

for each $\mathbf{x}$. We also add the normalization $\int_{\partial \Omega} N(\mathbf{x}, \mathbf{y}) \, ds_{\mathbf{y}} = 0$.

From equation (15) we that at any point $\mathbf{p} \in \Omega$ we thus have

$$\begin{aligned}
\nabla u_0(\mathbf{p}) \cdot \mathbf{n} &= \int_{\partial \Omega} \left(\nabla_x N(x_1, x_2, y_1, y_2) \cdot \mathbf{n} \right) g(y_1, y_2) \, ds_y \\
&= \int_{\partial \Omega} \frac{\partial N}{\partial \mathbf{n}_x}(x_1, x_2, y_1, y_2) \, g(y_1, y_2) \, ds_y
\end{aligned}$$

where $\frac{\partial N}{\partial \mathbf{n}_x} = \nabla_x N \cdot \mathbf{n}$. Parameterize the boundary by $y_1 = a(t)$, $y_2 = b(t)$, $t = 0 \ldots \tau$, and consider the gradient measured at the point $(x_1, x_2) = (p_1, p_2)$, the midpoint of the crack, so that

$$\begin{aligned}
\nabla u_0(p_1, p_2) \cdot \mathbf{n} &= \int_0^\tau \frac{\partial N}{\partial \mathbf{n}_x}(p_1, p_2, a(t), b(t)) \, g(a(t), b(t)) \, dt \\
&= \int_0^\tau f(t) g(t) \, dt
\end{aligned}$$

where $f(t) = \frac{\partial N}{\partial \mathbf{n}_x}(p_1, p_2, a(t), b(t))$ and $g(t) = g(a(t), b(t))$. Then our optimization problem may be stated as follows.

$$\max_{G \in L^2(\partial \Omega)} \int_0^\tau f(t) g(t) \, dt \tag{19}$$

subject to

$$\int_0^\tau g(t) s'(t) \, dt = 0 \tag{20}$$

$$\int_0^\tau |g(t)|^2 s'(t) \, dt = 1 \tag{21}$$

where $s'(t) = \sqrt{(a'(t))^2 + (b'(t))^2}$. Here we take $M = 1$ and $f(t)$ to be known.

10

We proceed by methods of Calculus of Variations. We transform (19), (20), and (21) into a single maximization problem by considering the functional $\int_0^\tau f(t)g(t) + \lambda_1 s'(t)g(t) + \lambda_2 s'(t)g(t)^2\, dt$. Let $F(t, g, g') = f(t)g(t) + \lambda_1 s'(t)g(t) + \lambda_2 s'(t)g(t)^2$, so that the Euler-Lagrange Equation, $\frac{\partial F}{\partial g} - \frac{d}{dt}\frac{\partial F}{\partial g'} = 0$, becomes simply $f(t) + \lambda_1 s'(t) + 2\lambda_2 s'(t)g(t) = 0$, so that

$$g(t) = -\frac{1}{2}\frac{f(t) + \lambda_1 s'(t)}{\lambda_2 s'(t)} \tag{22}$$

Imposing (20) and (21) we obtain

$$\lambda_1 = -\frac{1}{|\partial\Omega|}\int_0^\tau f(t)\, dt \tag{23}$$

$$\lambda_2 = \pm\frac{1}{2}\sqrt{\int_0^\tau \frac{(f(t) + \lambda_1 s'(t))^2}{s'(t)}\, dt} \tag{24}$$

Where we choose the sign of λ_2 so that the integral is maximized (this method provides stationary points, which may be maxima, minima, or simply saddle points).

As a simple example, suppose Ω is the unit disk parameterized in the usual way, $x_1(t) = \cos(t), x_2(t) = \sin(t)$, with $\tau = 2\pi$ and hence $s'(t) \equiv 1$. Also with Ω as the unit disk with $\mathbf{y} \in \partial\Omega$ we have $N(\mathbf{p}, \mathbf{y}) = 2\Gamma(\mathbf{p}, \mathbf{y})$ and $\nabla_x N(\mathbf{p}, \mathbf{y}) = 2\nabla_x\Gamma(\mathbf{p}, \mathbf{y})$. Also, suppose that a single crack, σ lies inside of Ω such that $\mathbf{p} = (0, 0)$, $\theta = 0$, and $\mathbf{n} = <0, 1>$. Then

$$\begin{aligned}
f(t) &= 2\nabla_x\Gamma(p_1 - \cos(t), p_2 - \sin(t)) \cdot \mathbf{n} \\
&= 2\frac{\partial\Gamma}{\partial x_2}(-\cos(t), -\sin(t)) \\
&= \frac{1}{\pi}\sin(t)
\end{aligned}$$

Therefore, we have from equations (23) and (24) that $\lambda_1 = 0$, $\lambda_2 = \frac{1}{2\sqrt{\pi}}$, and from (22) $g = \pm\frac{1}{\sqrt{\pi}}\sin(t)$. This is for a single crack σ, with $\mathbf{p} = (0, 0)$ and $\theta = 0$. The plus sign on g maximizes the gradient at $\mathbf{p}$, the minus sign minimizes (though both have the same magnitude). Of course this makes perfect sense—the optimal flux induces an interior flux which is straight down, orthogonal to the crack itself.

We can see that when the Neumann Kernel is known, the optimal heat flux is easy to compute. But in many regions actually finding the Neumann Kernel is not practical. We therefore would like to find a way to find g without explicitly computing the Neumann Kernel everywhere in Ω.

We need to compute $f(t) = \frac{\partial N}{\partial \mathbf{n}_x}(\mathbf{p}, \mathbf{y}(t))$ for a fixed $\mathbf{p} \in \Omega$ and all $\mathbf{y}(t) \in \partial\Omega$. We return to (17) and (18). First recall that $N(\mathbf{p}, \mathbf{y}) = \Gamma(\mathbf{p}, \mathbf{y}) + N_0(\mathbf{p}, \mathbf{y})$, and so

$$\frac{\partial N}{\partial \mathbf{n}_x}(\mathbf{p}, \mathbf{y}) = \frac{\partial\Gamma}{\partial \mathbf{n}_x}(\mathbf{p}, \mathbf{y}) + \frac{\partial N_0}{\partial \mathbf{n}_x}(\mathbf{p}, \mathbf{y}).$$

11

Now $\frac{\partial \Gamma}{\partial n_x}(\mathbf{p}, \mathbf{y})$ is simple to compute, since Γ is given in closed form. To find $\frac{\partial N_0}{\partial n_x}(\mathbf{p}, \mathbf{y})$ we simply note that $\frac{\partial N_0}{\partial n_x}(\mathbf{p}, \mathbf{y})$ must satisfy

$$\triangle_y \left(\frac{\partial N_0}{\partial n_x} \right) = 0 \text{ in } \Omega \tag{25}$$

$$\frac{\partial}{\partial m_y} \left(\frac{\partial N_0}{\partial n_x} \right) = -\frac{\partial^2 \Gamma}{\partial n_x \partial m_y} \text{ on } \partial\Omega \tag{26}$$

where switching the order of the differential operators is valid since $\mathbf{y}$ runs along the boundary and $\mathbf{p}$ is in the interior, so Γ and N_0 are C^∞ (recall that all functions are evaluated at $\mathbf{x} = \mathbf{p}$). Equations (25)-(26) can be easily solved numerically, and to obtain g we simply add the solution to $\frac{\partial \Gamma}{\partial n_x}(\mathbf{p}, \mathbf{y})$, which is easily computable. Thus we have that for any arbitrary region Ω, the optimal heat flux g exists and can be computed by numerically solving a straightforward boundary value problem.

4 Generalization to Multiple Cracks

4.1 The Algorithm

The locations of any n number of cracks were approximated in [4] by Bryan and Vogelius using a Newton-like method. This algorithm relied on solving a boundary value problem at each iteration, creating cumbersome computations. We instead base our reconstructions on equation (5), or rather, a close approximation. Specifically, as we did in deriving equation (7), we may approximate the contribution of each crack on the right in (5) and obtain the approximation

$$\alpha(\mathbf{x}) \approx \sum_{i=1}^{n} J_i \frac{(\mathbf{x} - \mathbf{p}_i, \mathbf{n}_{\sigma_i})}{(\mathbf{x} - \mathbf{p}_i, \mathbf{x} - \mathbf{p}_i)}. \tag{27}$$

This assumes that the cracks are not too close to the boundary, and "well-separated."

We will write $\alpha(\mathbf{x}, \{\mathbf{p}_i, \theta_i, J_i \mid i \leq n\})$ to denote the dependence of α on these parameters and use $\alpha^*(\mathbf{x})$ to denote the "true" value of α derived from measured data for a set of "true" cracks. We will define

$$F(\mathbf{x}) = \alpha(\mathbf{x}, \{\mathbf{p}_i, \theta_i, J_i \mid i \leq n\}) - \alpha^*(\mathbf{x}) \tag{28}$$

for $\mathbf{x} \in \partial\Omega$.

For the multiple crack problem we have not found any simple analytical method for locating the cracks. Instead we employ a least-squares approach using the function F. Specifically, we make an initial guess at the parameters of all n cracks (n itself may also be a guess). We "collect" measured data to compute $\alpha^*(\mathbf{x})$ and then $\alpha(\mathbf{x})$ is computed using the

12

initial guess at the parameters of the n cracks. After the initial guess is made, the Levenberg-Marquardt Method is used to adjust the parameters until $\sum\limits_{j=1}^{m} F(\mathbf{x}_j)^2$ is minimized, where $\mathbf{x}_j$ denotes the jth point of a list of m data points on the boundary $\partial\Omega$

Ideally $F(\mathbf{x}_j)$ should be zero for each $\mathbf{x}_j \in \partial\Omega$ when the correct $\mathbf{p}_i, \theta_i$, and J_i value have been obtained for each σ_i. However, due to the various assumptions made this is typically note the case. After the optimization algorithm terminates we will have an approximation to each crack midpoint $\mathbf{p}_i$, angle θ_i, and jump integral J_i. Finally, using the approximation (11) we can approximate each L_i. In order to obtain the best approximation of the location of the cracks, the initial guess should have the n cracks well separated.

Note that this approach does NOT involve solving any boundary value problems.

4.2 Numerical Examples

Provided in this section are a variety of numerical examples of estimating the location of two or more perfectly insulating, pair-wise disjoint cracks. Aside from the number of cracks, the situation is identical to that of the single crack example, e.g., input flux $g(t) = \sin(t)$. The examples in this section demonstrates the relative importance of knowledge of the number of cracks contained inside of Ω before estimating the locations of the cracks, an issue which has been examined from a statistical point of view in [1].

In the first example, two actual cracks were used to generate the data and α^* was computed. To solve the inverse problem, initial parameters were entered into a Levenberg-Marquardt C program specifically designed for locating two cracks, with no prior knowledge of the locations of the two actual cracks used to generate u and α^* for $\mathbf{x} \in \partial\Omega$. The locations of the cracks were recovered after 23 iterations, which yielded a minimum F^2 value of 0.000108. Then, using the recovered parameters for the two cracks, the program was run again, and the same parameters were obtained again after 7 iterations, again with a minimum F^2 value of 0.000108. As shown in Figure 4, the reconstructed cracks essentially coincide with the actual cracks.

In the second example we use the same two "real" cracks to general α^*, then attempt to solve the inverse problem under the assumption that three cracks are present. Initial parameters were entered into a C program specifically designed for locating three cracks with no prior knowledge of the locations of the two cracks used to generate the boundary data. The locations of the 'three' cracks were recovered after 1000 iterations, when the program was designed to terminate. Although this seems like a tremendous amount of computations, the program was complete within two minutes. The minimum F^2 value obtained was 0.000017, which indicates that a very good approximation of the locations of the cracks should have been obtained. However, as shown in Figure 5, a single crack is approximated by the intersection of two cracks, whose endpoints lie very close to the endpoints of the actual crack.
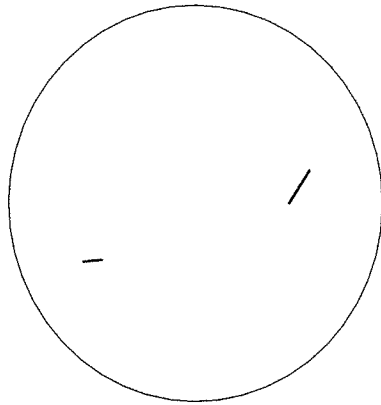
13

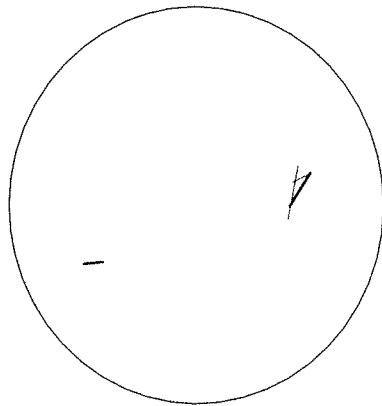Figure 4: Reconstruction of two perfectly insulating, pair-wise disjoint cracks.

Figure 5: Reconstruction of two perfectly insulating, pair-wise disjoint cracks, using a program specific to locating exactly three cracks and arbitrary initial parameters.
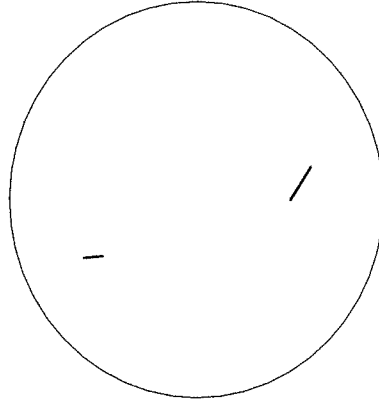
Figure 6: Reconstruction of two perfectly insulating, pair-wise disjoint cracks, using a program specific to locating three cracks

In the third example we again attempt to fit three cracks to data general by only two cracks. The first two sets of initial parameters used were close to the actual parameters of the two cracks used to generate the boundary data. The last set of parameters used were relatively far away from the first set. After only 11 iterations, the minimum F^2 value of 0.000108 was obtained, the first two cracks essentially coincided with the actual cracks and the third crack was shrunk to a length of $\approx$ .00495 and its midpoint was far outside of the region, at $\approx (-3.24, 0.074)$. This third crack is omitted from the reconstruction diagram, shown in Figure 6.

We now provide some examples in which three actual cracks are used to generate the forward data. In this next example, initial parameters for three guessed cracks were entered into a C program specifically designed for estimating three cracks with no prior knowledge of the locations of the cracks used to generate $u(\mathbf{x})$ for $\mathbf{x} \in \partial\Omega$. The locations of the cracks were recovered after 99 iterations. Then, using the recovered parameters for the three cracks, the program was run again, and parameters identical to the previous values were obtained after 38 iterations. As shown in Figure 7, the reconstructed cracks act as a fair estimation of the actual cracks. However, in this example, the minimum F^2 value obtained is 0.00488, indicating that the final approximation is not as good as the approximation locating two cracks in the first example of the previous section. However, as can be seen in Figure 7, the assumption that the length of each crack is much less than the distance from the midpoint of the crack to any point on the boundary is violated. Taking this fact into account, this method of approximating the location of perfectly insulating cracks seems reasonably good.

We would like to note at this point that each C program approximating the locations of two and three cracks was completed nearly instantly, except for the second example, which was able to complete 1000 iterations in less than two minutes. However in the specific
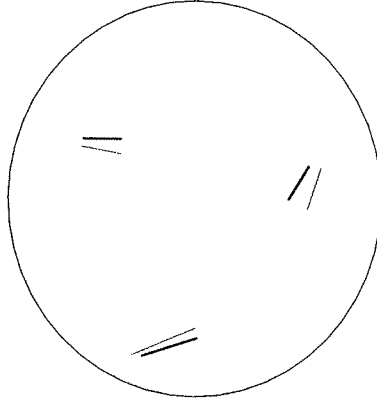
Figure 7: Reconstruction of three perfectly insulating, pairwise disjoint cracks

programs used to obtain the approximations of the locations, the precision was far too stringent, as the program failed to terminate immediately when recovered parameters had been entered as an initial guess. Relaxing the precision slightly would reduce the number of iterations the program would have to traverse before finding an appropriate approximation.

5   Relating Crack Length and Jump Integral

The goal of this section is prove the relation

$$\int_\sigma [u]\, ds = \frac{\pi}{4}(\nabla u_0(\mathbf{p}) \cdot \mathbf{n})|\sigma|^2 + O(|\sigma^3|) \tag{29}$$

from which we derived equation (11) used in the reconstruction process.

5.1   Reduction to an Integral Equation

In what follows we will use u_0 to denote the harmonic function on the "uncracked" domain Ω with Neumann data g, while u denotes the solution to (1)-(3). A central portion of our reconstruction algorithm for estimating crack length concerns the relationship between the jump integral $\int_\sigma [u]\, ds$ over a typical crack σ, the length of σ, and u_0. We now prove the relation (11).

For the moment we assume that Ω contains a single linear insulating crack σ. Via translation and rotation, we may suppose that Ω contains a neighborhood of the origin, and that the crack σ lies inside of Ω on the interval $(0, \epsilon)$ on the x-axis, for some $\epsilon > 0$. Let the unit normal vector to σ be given by $\mathbf{n}_\sigma = <0, 1>$.

We will let Γ denote the Green's Function for the Laplacian operator in $\mathbb{R}^2$, given by

16

$$\Gamma(x_1, x_2) = -\frac{1}{4\pi} \log(x_1^2 + x_2^2) \tag{30}$$

Lemma 1 *Let $v(x, y) = \int_0^\epsilon \frac{\partial \Gamma}{\partial y}(x - s, y)\phi(s)ds$ for some $\phi \in C^2(0, \epsilon) \cap C^0([0, \epsilon])$ with $\phi(0) = \phi(\epsilon) = 0$. Then $v(x, y)$ is harmonic away from σ, $\frac{\partial v}{\partial y}$ is continuous over σ, and $[v](x, y) = \phi(x, y)$ for all $(x, y) \in \sigma$.*

Proof. First note that if (x, y) is not near σ, the integrand is perfectly smooth. Because the integral is over a finite region, the operator $\frac{\partial^2}{\partial x^2} + \frac{\partial^2}{\partial y^2}$ can be interchanged with the integral. Then we have that

$$
\begin{aligned}
\left(\frac{\partial^2}{\partial x^2} + \frac{\partial^2}{\partial y^2} \right) \frac{\partial \Gamma}{\partial y}(x - s, y) &= -\frac{y(2x - 2s)^2}{\pi((x - s)^2 + y^2)^3} + \frac{y}{\pi((x - s)^2 + y^2)^2} \\
&+ \frac{3y}{\pi((x - s)^2 + y^2)^2} - \frac{4y^3}{((x - s)^2 + y^2)^3} \\
&= 0
\end{aligned}
$$

for $x - s \neq y$. Thus we have that v is harmonic at any (x, y) away from σ.

Written out explicitly we have

$$v(x, y) = \int_0^\epsilon -\frac{1}{2\pi} \frac{y}{(x - s)^2 + y^2} \phi(s) \, ds \tag{31}$$

so the integrand is perfectly smooth for all (x, y) away from σ. Also, as the integrand is over a finite interval, we can differentiate under the integral to obtain

$$\frac{\partial v}{\partial y}(x, y) = -\frac{1}{2\pi} \int_0^\epsilon \frac{(x - s)^2 - y^2}{((x - s)^2 + y^2)^2} \phi(s) ds. \tag{32}$$

From this, it is evident that if the limit as $y \to 0^-$ exists, then $\lim_{y \to 0^-} \frac{\partial v}{\partial y} = \lim_{y \to 0^+} \frac{\partial v}{\partial y}$, as y only appears in squared form.

We will show that $\lim_{y \to 0} \frac{\partial v}{\partial y}$ exists. Employing integration by parts yields

$$\int_0^\epsilon \frac{(x - s)^2 - y^2}{((x - s)^2 + y^2)^2} \phi(s) ds = \int_0^\epsilon \frac{x - s}{((x - s)^2 + y^2)} \phi'(s) ds \tag{33}$$

as we have $\phi(s) \in L^2(0, \epsilon)$ and $\phi(0) = \phi(1) = 0$ by assumption. Now, for any $\eta > 0$, we have

$$\lim_{y \to 0} \int_0^{x - \eta} \frac{x - s}{(x - s)^2 + y^2} \phi'(s) ds = \int_0^{x - \eta} \frac{\phi'(s)}{x - s} ds$$

$$\lim_{y \to 0} \int_{x + \eta}^\epsilon \frac{x - s}{(x - s)^2 + y^2} \phi'(s) ds = \int_{x + \eta}^\epsilon \frac{\phi'(s)}{x - s}$$

as the integrands on the left converge uniformly to those on the right over the ranges of integration. Again by integration by parts, we also have that

$$\int_{x-\eta}^{x+\eta} \frac{x-s}{(x-s)^2+y^2}\phi'(s)ds = \frac{1}{2}\int_{x-\eta}^{x+\eta}\phi''(s)\log((x-s)^2+y^2)ds. \tag{34}$$

By assumption, $|\phi''(s)| \leq M$ for $s \in (x-\eta, x+\eta)$, and if we let $\psi(x, y, \eta)$ denote the quantity in the right hand side of (34), we have

$$
\begin{aligned}
|\psi(x, y, \eta)| &\leq \frac{M}{2}\int_{x-\eta}^{x+\eta}|\log((x-s)^2+y^2)|ds \\
&= M|\eta\log(y^2+\eta^2) - 2\eta + 2y\arctan(\frac{\eta}{y})| \\
&\leq M|\eta\log(y^2+\eta^2 - 2) + \pi|y||,
\end{aligned}
$$

as $\|\arctan\|_\infty \leq \frac{\pi}{2}$. Therefore, we have that

$$
\begin{aligned}
\int_0^\epsilon \frac{x-s}{(x-s)^2+y^2}\phi'(s)ds &= \int_0^{x-\eta}\frac{x-s}{(x-s)^2+y^2}\phi'(s)ds \\
&+ \int_{x-\eta}^{x+\eta}\frac{x-s}{(x-s)^2+y^2}\phi'(s)ds \\
&+ \int_{x+\eta}^\epsilon\frac{x-s}{(x-s)^2+y^2}\phi'(s)ds
\end{aligned}
$$

and taking the limit as $y \to 0$ yields

$$\lim_{y\to 0}\int_0^\epsilon \frac{x-s}{(x-s)^2+y^2}\phi'(s)ds = \int_0^{x-\eta}\frac{\phi'(s)}{x-s}ds + \int_{x+\eta}^\epsilon\frac{\phi'(s)}{x-s}ds + E(\eta)$$

where $|E(\eta)| \leq 2\eta M(\log(\eta) + 1)$. Verification that $\lim_{\eta\to 0} E(\eta) = 0$ is left to the reader, leaving us with

$$\frac{\partial v}{\partial y}|_\sigma = \frac{1}{2\pi}\lim_{y\to 0}\int_0^\epsilon \frac{x-s}{(x-s)^2+y^2}\phi'(s)ds = \frac{1}{2\pi}\text{p.v.}\int_0^\epsilon \frac{\phi'(s)}{x-s}ds. \tag{35}$$

It is a rather standard exercise to verify that the principal integral on the right above exists for $x \in (0, \epsilon)$, since ϕ is C^2 (and hence ϕ' is C^1) on the interval $(0, \epsilon)$. Therefore, by (32) and (33), we have that $\frac{\partial v}{\partial y}$ is continuous over σ.

Finally, we examine $[u]$ across σ. For any fixed $\delta > 0$, as $y \to 0$, $\frac{y}{(x-s)^2+y^2}\phi(s)$ converges uniformly to zero for $s \in (0, x-\delta)$ and for $s \in (x+\delta, \epsilon)$, which shows that

$$\lim_{y\to 0^+} -\frac{1}{2\pi}\int_0^{x-\delta}\frac{y}{(x-s)^2+y^2}\phi(s)ds$$

18

$$= \lim_{y \to 0^+} -\frac{1}{2\pi} \int_{x+\delta}^{\epsilon} \frac{y}{(x-s)^2 + y^2} \phi(s) ds$$
$$= 0$$

for any $\delta > 0$. It follows directly that

$$v^+(x, y) = -\frac{1}{2\pi} \lim_{y \to 0^+} \int_{x-\delta}^{x+\delta} \frac{y}{(x-s)^2 + y^2} \phi(s) ds \tag{36}$$

for any fixed $\delta > 0$.

Because ϕ is continuous by assumption, for any $\eta > 0$, there exists $\delta > 0$ such that $|\phi(x) - \phi(s)| < \eta$ if $|x - s| < \delta$. Therefore, we have

$$\left| \int_{x-\delta}^{x+\delta} \frac{y}{(x-s)^2 + y^2} \phi(s) ds - \phi(x) \int_{x-\delta}^{x+\delta} \frac{y}{(x-s)^2 + y^2} ds \right|$$

$$\leq \eta \int_{x-\delta}^{x+\delta} \frac{y}{(x-s)^2 + y^2} ds \tag{37}$$

$$= \eta 2 \arctan(\frac{\delta}{y})$$

$$\leq \eta \pi.$$

Multiplication of (37) by $-\frac{1}{2\pi}$ yields

$$\left| \frac{1}{2} \phi(x) - \frac{1}{2\pi} \int_{x-\delta}^{x+\delta} \frac{y}{(x-s)^2 + y^2} \phi(s) ds \right| \leq \frac{\eta}{2}$$

for any y. Then, taking the limit as $y \to 0$ shows,

$$\lim_{y \to 0^+} \frac{1}{2\pi} \int_{x-\delta}^{x+\delta} \frac{y}{(x-s)^2 + y^2} \phi(s) ds = \frac{1}{2} \phi(x)$$

which, along with (10), gives us that $v^+(x, y) = \frac{1}{2} \phi(x)$. A similar argument shows that $v^-(x, y) = -\frac{1}{2} \phi(x)$, so it follows directly that

$$[v](x, 0) = \phi(x), \text{ for } (x, 0) \in \sigma \tag{38}$$

thereby completing the proof. $\square$

We will use the preceding Lemma to construct an approximate solution $\tilde{u} \approx u$ to equations (1)-(3), by choosing $\phi(s)$ so that $\frac{\partial v}{\partial \mathbf{n}_\sigma} = -\frac{\partial u_0}{\partial \mathbf{n}_\sigma}$ on σ. It then follows that the function $\tilde{u} = u_0 + v$

19

satisfies $\frac{\partial v}{\partial \mathbf{n}} = 0$ on σ, and moreover, we will show that $\int_\sigma [\tilde{u}] = \int_\sigma [u] + O(\epsilon^3)$. Since we can compute $\int_\sigma [\tilde{u}] = \frac{\pi}{4}\epsilon^2(\nabla u_0 \cdot \mathbf{n})$ directly, the approximation $\int_\sigma [u] \approx \frac{\pi}{4}\epsilon^2(\nabla u_0 \cdot \mathbf{n}) + O(\epsilon^3)$ will follow.

From Lemma 1, choosing a function α defined on $[0, \epsilon]$ so that $v(x, y) = \int_0^\epsilon \frac{\partial \Gamma}{\partial y}(x - s, y)\alpha(s)ds$ satisfies $\frac{\partial v}{\partial \mathbf{n}_\sigma} = -\frac{\partial u_0}{\partial \mathbf{n}_\sigma}$ requires that we solve

$$\text{p.v.} \int_0^\epsilon \frac{\alpha'(s)}{x - s}\, ds = -2\pi \frac{\partial u_0}{\partial y}(x) \tag{39}$$

for $0 < x < \epsilon$, where we assume the crack is the interval $(0, \epsilon)$ on the x axis. In fact, in what follows we will write σ_ϵ when we need to emphasize the crack's dependence on ϵ. The function u_0 is smooth near σ_ϵ, and we can write

$$
\begin{aligned}
\frac{\partial u_0}{\partial y}(x, 0) &= \frac{\partial u_0}{\partial y}(p, 0) + \frac{\partial^2 u_0}{\partial x \partial y}(q(x), 0)(x - p) \\
&= \frac{\partial u_0}{\partial y}(p, 0) + \epsilon R(x)
\end{aligned}
$$

where $p = \epsilon/2$ is the midpoint of σ_ϵ, $q(x)$ denotes some number between p and x, and $R(x) = (\frac{x-p}{\epsilon})\frac{\partial^2 u_0}{\partial x \partial y}(q(x), 0)$. Note that R, as well as its derivatives of any order, can be bounded in terms of $\|g\|_{L^2(\partial\Omega)}$.

The solution α to equation (40) is given as $\alpha(s) = -2\pi\frac{\partial u_0}{\partial y}(p, 0)\phi(s)$ where ϕ satisfies

$$\text{p.v.} \int_0^\epsilon \frac{\phi'(s)}{x - s}\, ds = 1 + \epsilon r(x) \tag{40}$$

with $r(x) = R/(\partial u_0(p)/\partial y)$, provided that p is not a critical point for u_0.

5.2   Solvability of the Integral Equation

We wish to solve (40) for ϕ, and we wish $\phi \in L_2(0, 1)$. First we must justify that (40) has a unique $L_2(0, 1)$ solution. To do so we will establish three preliminary facts.

Fact 1 *If $\{\phi_n\}_0^\infty \subset L_2(0, \pi)$ is orthonormal and complete, $\{\mu_n\}_0^\infty \subset \mathbb{R}$ and $k(x, t) = \sum_{n=0}^\infty \mu_n \phi_n(x)\overline{\phi_n(t)}$, then $\{\phi_n\}$ is a complete set of eigenvectors and $\{\mu_n\}$ is the corresponding set of eigenvalues for the $L_2[0, \pi]$ operator K defined by $(K\phi)(x) = \int_0^\pi k(x, t)\phi(t)\, dt$.*

Proof For all $\phi \in L_2(0, \pi)$,

20

$$
\begin{aligned}
(K\phi)(x) &= \int_0^\pi k(x,t)\phi(t)\,dt \\
&= \int_0^\pi \left[\sum_{n=0}^\infty \mu_n \phi_n(x)\overline{\phi_n(t)} \right] \phi(t)\,dt \\
&= \sum_{n=0}^\infty \mu_n \phi_n(x) \int_0^\pi \phi(t)\overline{\phi_n(t)}\,dt \\
&= \sum_{n=0}^\infty \mu_n \phi_n(x)(\phi, \phi_n)
\end{aligned}
$$

So

$$
K\phi = \sum_{n=0}^\infty \mu_n \phi_n(\phi, \phi_n)
$$

Now for $m = 0, 1, \ldots$, ϕ_m is in $L_2(0,\pi)$, and $(\phi_m, \phi_n) = \begin{cases} 0 & if \quad m \neq n \\ 1 & if \quad m = n \end{cases}$, since $\{\phi_n\}_0^\infty$ is orthonormal. Thus

$$
K\phi_m = \sum_{n=0}^\infty \mu_n \phi_n(\phi_m, \phi_n) = \mu_m \phi_m
$$

So $K\phi_m = \mu_m \phi_m$, and thus $\{\phi_n\}_0^\infty$ are a complete set of eigenvectors of K, and $\{\mu_m\}_0^\infty$ are the corresponding eigenvalues. $\square$

Fact 2 *Let $\{\phi_n\}_0^\infty \subset L_2(0,\pi)$ be complete and orthonormal, $\{\mu_n\}_0^\infty \subset \mathbb{R}\backslash\{0\}$ be the eigenvectors and eigenvalues of a compact and self-adjoint operator K on $L_2(0,\pi)$. Then for $g \in L_2(0,\pi)$, $K\phi = g$ has a unique $L_2(0,\pi)$ solution if $\sum_{n=0}^\infty |\frac{1}{\mu_n}(g, \phi_n)|^2 < \infty$, in which case the solution is given by $\phi = \sum_{n=0}^\infty \frac{1}{\mu_n}(g, \phi_n)\phi_n$.*

Proof For all $x \in \mathbb{R}$, let $\phi(x) = \sum_{n=0}^\infty \frac{1}{\mu_n}(g, \phi_n)\phi_n(x)$. Now

$$
\begin{aligned}
\int_0^\pi |\phi(x)|^2\,dx &= \int_0^\pi |\sum_{n=0}^\infty \frac{1}{\mu_n}(g, \phi_n)\phi_n(x)|^2\,dx \\
&\leq \int_0^\pi \left(\sum_{n=0}^\infty |\frac{1}{\mu_n}(g, \phi_n)\phi_n(x)| \right)^2 dx
\end{aligned}
$$

$$\leq \int_0^\pi \sum_{n=0}^\infty |\frac{1}{\mu_n}(g,\phi_n)\phi_n(x)|^2 \, dx$$

$$= \sum_{n=0}^\infty \int_0^\pi |\frac{1}{\mu_n}(g,\phi_n)\phi_n(x)|^2 \, dx$$

$$= \sum_{n=0}^\infty |\frac{1}{\mu_n}(g,\phi_n)|^2 \int_0^\pi |\phi_n(x)|^2 \, dx$$

$$= \sum_{n=0}^\infty |\frac{1}{\mu_n}(g,\phi_n)|^2$$

$$< \infty$$

Thus $\int_0^\pi |\phi(x)|^2 \, dx < \infty$, so $\phi \in L_2(0,\pi)$. Now,

$$K\phi = K\left(\sum_{n=0}^\infty \frac{1}{\mu_n}(g,\phi_n)\phi_n\right)$$

$$= \sum_{n=0}^\infty \frac{1}{\mu_n}(g,\phi_n)K\phi_n$$

$$= \sum_{n=0}^\infty \frac{\mu_n}{\mu_n}(g,\phi_n)\phi_n$$

$$= \sum_{n=0}^\infty (g,\phi_n)\phi_n$$

But since $\{\phi_n\}$ is complete, $g = \sum_{n=0}^\infty (g,\phi_n)\phi_n$, so $K\phi = g$. Thus ϕ solves $K\phi = g$. $\square$

Fact 3 *Let K be an operator from $L_2(0,\pi)$ to $L_2(0,\pi)$ defined by*

$$(K\hat\psi)(\sigma) = \int_0^\pi \log|\cos(\sigma) - \cos(\theta)|\hat\psi(\theta) \, d\theta \tag{41}$$

For $(0 < \sigma < \pi)$. Then the eigenvalues of K are $\mu_0 = -\pi\log(2)$, $\mu_n = -\frac{\pi}{n}$ for $n \geq 1$, and the eigenfunctions are $\phi_0 = \frac{1}{\sqrt{\pi}}$, $\phi_n(\sigma) = \sqrt{\frac{2}{\pi}}\cos(n\sigma)$, $n \geq 1$, which are orthonormal and complete in $L_2(0,\pi)$.

Proof One can verify that the kernel of this integral operator can be written

$$\log|\cos(\sigma) - \cos(\theta)| = -\log 2 - \sum_{i=1}^\infty \frac{2\cos(n\sigma)\cos(n\theta)}{n}$$

$$(0 \leq \theta, \sigma \leq pi, \theta \neq \sigma)$$

22

(see Porter and Stirling, Appendix C, and example 6.10). This is of the form $\sum_{n=0}^{\infty} \mu_n \phi_n(\sigma) \overline{\phi_n(\theta)}$ with $\mu_0 = -\pi log(2)$, $\mu_n = -\frac{\pi}{n}$, and $\phi_0 = \frac{1}{\sqrt{\pi}}$, $\phi_n(\sigma) = \sqrt{\frac{2}{\pi}} \cos(n\sigma)$. It is easy to verify that $\{\phi_n\}$ is orthonormal and complete in $L_2(0, \pi)$. We then employ Fact 1 to conclude that $\{\phi_n\}$ are the eigenvectors of K, and $\{\mu_n\}$ are the eigenvalues. $\square$

The following Theorem shows that equation (40) has a unique solution.

Lemma 2 *Let $f \in C^3[0, 1]$ and $\delta > 0$ a real constant. Then the integral equation*

$$\text{p.v.} \int_0^1 \frac{\phi'(t)}{t - s} \, dt = 1 + \delta f(s), \quad 0 < s < 1, \tag{42}$$

has a unique solution ϕ of the form

$$\phi(t) = -\frac{1}{\pi} \sqrt{t - t^2} + \delta \psi_1(t)$$

which is continuous on $[0, 1]$, twice continuously-differentiable on $(0, 1)$, with ϕ' integrable on $(0, 1)$ and $\phi(0) = \phi(1) = 0$. Also, $\|\psi_1\|_\infty$ is bounded by $\|f\|_{C^3[0,1]}$.

Note that for such a function the principle value integral will exist for each $s \in (0, 1)$ since ϕ' is continuously differentiable.

To prove the Lemma we cast equation (42) into an alternate form. Consider a function $\phi(t)$ with the above stated regularity which satisfies equation (42). We proceed as in section 9.5.2 of [7]: Integrate both sides of equation (42) in s from $s = 0$ to $s = x$ to obtain

$$-\int_0^1 \ln(2|x - t|)\phi'(t) \, dt = x + \delta \int_0^x f(s) \, ds - C_1 \tag{43}$$

for a constant $C_1 = \int_0^1 \ln(2s)\phi'(s) \, ds$, where the legitimacy of the integration and swapping of order is justified by equation (9.12) and Lemma 9.1 in [7], and the constant C_1 may be considered arbitrary. Any solution to equation (42) with the stated regularity satisfies equation (43). Conversely, as shown in that text (again, section 9.5.2) any solution to (43) also satisfies (42).

Now integrate by parts on the left in equation (43) to transfer the derivative off of ϕ, taking care to interpret the resulting principal value terms correctly (briefly, split the integral into pieces over intervals $(0, x - \epsilon)$ and $(x + \epsilon, 1)$, integrate by parts on each, then take the limit as $\epsilon \to 0$) and use $\phi(0) = \phi(1) = 0$ to obtain

$$\text{p.v.} \int_0^1 \frac{\phi(t)}{t - x} \, dt = x + \delta F(x) - C_1 \tag{44}$$

23

where $F(x) = \int_0^x f(s)\,ds$. One can also easily verify that any solution to equation (44) necessarily satisfies equation (43), provided ϕ has the required regularity.

Again following section 9.5.2 in [7], integrate both sides of equation (44) in x from $x = 0$ to $x = y$ to obtain

$$-\int_0^1 \ln(2|y-t|)\phi(t)\,dt = \frac{1}{2}y^2 + \delta\int_0^y F(t)\,dt - C_1 y + C_2 \tag{45}$$

in which C_2 may be considered a second arbitrary constant at our disposal. An argument similar to that which showed the equivalence of equations (42) and (43) also shows the equivalence of equations (44) and (45). We will show that equation (45), and hence equation (42), possesses a unique solution with the required regularity and $\phi(0) = \phi(1) = 0$.

As in [7] we make the (invertible) substitution $y = \cos^2(\sigma/2)$, $t = \cos^2(\theta/2)$ and obtain

$$-\int_0^\pi \ln|\cos(\theta) - \cos(\sigma)|\hat{\phi}(\theta)\,d\theta = g(\sigma) \tag{46}$$

for $0 < \sigma < \pi$, where $\hat{\phi}(\theta) = \frac{1}{2}\phi(\cos^2(\theta/2))\sin(\theta)$ and

$$g(\sigma) = C_2 - C_1\cos^2(\sigma/2) + \frac{1}{2}\cos^4(\sigma/2) + \frac{\delta}{2}\int_\sigma^\pi F(\cos^2(\theta/2))\sin(\theta)\,d\theta.$$

By using $\cos^2(\sigma/2) = (1 + \cos(\sigma))/2$ we obtain

$$g(\sigma) = \left(C_2 - \frac{C_1}{2} + \frac{3}{16}\right) + \left(-\frac{C_1}{2} + \frac{1}{4}\right)\cos(\sigma) + \frac{1}{16}\cos(2\sigma) + \frac{\delta}{2}\int_\sigma^\pi F(\cos^2(\theta/2))\sin(\theta)\,d\theta.$$

Equation (46) can thus be written

$$(K\hat{\phi})(\sigma) = g(\sigma) \tag{47}$$

where K denotes the integral operator on the right side of equation (46), $g(\sigma) \equiv c_1 + c_2\cos(\sigma) + \frac{1}{16}\cos(2\sigma) + \delta G(\sigma)$ with $c_1 = -C_1/2 + C_2 + 3/16$, $c_2 = -C_1/2 + 1/4$, and

$$G(\sigma) = \frac{1}{2}\int_\sigma^\pi F((1 + \cos(\theta))/2)\sin(\theta)\,d\theta. \tag{48}$$

We will show that for any given choice of C_1 and C_2 equation (47) possesses a unique solution in $L^2(0, \pi)$, and that this solution can be used to recover the solution to equation (42).

To see this, we use Fact 3 from the previous section, that the operator K is compact and self-adjoint on $L^2(0, \pi)$, with eigenvalues $\mu_0 = \pi\ln(2)$, $\mu_n = \pi/n$ for $n \geq 1$, and orthonormal

24

eigenfunctions $\phi_0(\sigma) = 1/\sqrt{\pi}$, $\phi_n(\sigma) = \sqrt{2/\pi}\cos(n\sigma)$ for $n \geq 1$. By Fact 2 the unique $L^2(0,\pi)$ solution to equation (47) is thus given by

$$\begin{aligned}
\hat{\phi}(\sigma) &= \sum_{n=0}^{\infty} \frac{1}{\mu_n}(g, \phi_n) \\
&= \sum_{n=0}^{\infty} \frac{1}{\mu_n}(c_1 + c_2\cos(\sigma) + \frac{1}{16}\cos(2\sigma), \phi_n)\phi_n + \delta \sum_{n=0}^{\infty} \frac{1}{\mu_n}(G, \phi_n)\phi_n \\
&= \frac{c_1}{\pi\ln(2)} + \frac{c_2}{\pi}\cos(\sigma) + \frac{1}{8\pi}\cos(2\sigma) + \delta \sum_{n=0}^{\infty} \frac{1}{\mu_n}(G, \phi_n)\phi_n \qquad (49)
\end{aligned}$$

where $(\cdot, \cdot)$ denotes the L^2 inner product, provided the last sum on the right in (49) converges in $L^2(0, \pi)$. This requires

$$\sum_{n=1}^{\infty} (\frac{1}{\mu_n}(G, \phi_n))^2 < \infty. \qquad (50)$$

We now show that this is true, and that in fact the sum on the right in (49) actually represents a $C^2(0, \pi)$ function. With G as defined by equation (48) repeated integration by parts (taking derivatives off of $\sin(n\sigma)$ or $\cos(n\sigma)$, putting derivatives on G) shows that

$$\int_0^{\pi} G(\sigma)\cos(n\sigma)\, d\sigma = -\frac{1}{n^5}\int_0^{\pi} \sin(n\sigma)G^{(5)}(\sigma)\, d\sigma$$

since all endpoint terms at $\sigma = 0$ and $\sigma = \pi$ in each integration by parts fortuitously vanish. The function $G^{(5)}$ (which involves derivatives of f up the third order) is in $L^2(0, \pi)$, so that we find $\frac{1}{\mu_n}(G, \phi_n) = \frac{d_n}{n^4}$ with $d_n = -\sqrt{2/\pi^3}(G^{(5)}, \sin(n\sigma))$, and so $\sum_n d_n^2 < \infty$. As a result the sum

$$\sum_{n=1}^{\infty} \frac{1}{\mu_n}(G, \phi_n)\phi_n(\sigma) = \sqrt{2/\pi}\sum_{n=1}^{\infty} \frac{d_n}{n^4}\cos(n\sigma)$$

is in $L^2(0, \pi)$, and term-by-term differentiation shows the sum possesses a third derivative in $L^2(0, \pi)$, and hence a continuous second derivative on $[0, \pi]$. Thus the unique (for a given choice of C_1 and C_2) $L^2(0, \pi)$ solution $\hat{\phi}(\sigma)$ to equation (46) is given by

$$\hat{\phi}(\sigma) = \frac{c_1}{\pi\ln(2)} + \frac{c_2}{\pi}\cos(\sigma) + \frac{1}{8\pi}\cos(2\sigma) + \delta H(\sigma)$$

where

$$H(\sigma) = d_0 + \sum_{n=1}^{\infty} \frac{d_n}{n^4}\cos(n\sigma)$$

for the square-summable sequence $\{d_n\}$.

Note that if a $C[0,1]$ solution $\phi(y)$ to equation (42) exists, the corresponding function $\hat{\phi}$ satisfying equation (47) will certainly be in $L^2(0,\pi)$. Thus by considering equation (47), we can be sure to locate a $C[0,1]$ to equation (42) if it exists.

Use $\sigma = 2\arccos(\sqrt{y})$ to obtain

$$\hat{\phi}(\sigma) = \frac{c_1}{\pi\ln(2)} + \frac{c_2}{\pi}\cos(2\arccos(\sqrt{y})) + \frac{1}{8\pi}\cos(4\arccos(\sqrt{y})) + \delta H(2\arccos(\sqrt{y})).$$

Note that for $0 < y < 1$ we have $\cos(2\arccos(\sqrt{y})) = 2y - 1$ and $\cos(4\arccos(\sqrt{y})) = 8y^2 - 8y + 1$. With $y = \cos^2(\sigma/2)$ and $\hat{\phi}(\sigma) = \frac{1}{2}\phi(\cos^2(\sigma/2))\sin(\sigma)$ we have $\sin(\sigma) = 2\sqrt{y - y^2}$ so that

$$\phi(y) = \frac{\alpha(y)}{\sqrt{y - y^2}} \tag{51}$$

where

$$\alpha(y) = \frac{c_1}{\pi\ln(2)} + \frac{c_2}{\pi}(2y - 1) + \frac{1}{8\pi}(8y^2 - 8y + 1) + \delta\tilde{H}(y) \tag{52}$$

with $\tilde{H}(y) = H(2\arccos(\sqrt{y}))$. Also note that

$$\tilde{H}(y) = d_0 + \sum_{n=1}^{\infty}\frac{d_n}{n^4}\cos(2n\arccos(\sqrt{y})) = d_0 + \sum_{n=1}^{\infty}\frac{d_n}{n^4}T_n(2y - 1) \tag{53}$$

where T_n denotes the nth Chebyshev polynomial of the first kind, which can be defined by $T_n(x) = \cos(2n\arccos(\sqrt{(x+1)/2}))$ (easily derived from the well-known formula $T_n(x) = \cos(n\arccos(x))$ and the half-angle formula). Although $\hat{\phi}$ is in $L^2(0,\pi)$, this does not guarantee that $\phi(y)$ lies in $L^2(0,1)$. However, the latter is indeed guaranteed if the constants c_1 and c_2 (or C_1 and C_2) are chosen correctly, as shown below.

Before proceeding, note that the Chebyshev polynomials satisfy $\sup_{-1\leq x\leq 1}|T_n(x)| = 1$ and $\sup_{-1\leq x\leq 1}|T_n'(x)| = n^2$. Moreover, since $d_k = -\sqrt{2/\pi^3}(G^{(5)}, \sin(k\sigma))$ and $G^{(5)}$ can be easily bounded in terms of $\|f\|_{C^3}$, we have $|d_k| \leq C\|f\|_{C^3}$ for some constant C and all k. From (53) it is thus clear that $\tilde{H}(y)$ is continuous on $[0,1]$, and term-by-term differentiation of the right side of (53) shows that $\tilde{H}'(y)$ is also continuous on $[0,1]$. In particular, $\tilde{H}(y)$ is in $C^1[0,1]$, and hence so is $\alpha(y)$. Finally, note that

$$|\tilde{H}(y)| = \left|d_0 + \sum_{n=1}^{\infty}\frac{d_n}{n^4}T_n(2y-1)\right| \leq \sup_n|d_n|\sum_{n=1}^{\infty}\frac{1}{n^4} \leq C\|f\|_{C^3}. \tag{54}$$

and similarly

$$|\tilde{H}'(y)| = \left|\sum_{n=1}^{\infty}\frac{2d_n}{n^4}T_n'(2y-1)\right| \leq 2\sup_n|d_n|\sum_{n=1}^{\infty}\frac{1}{n^2} \leq C\|f\|_{C^3} \tag{55}$$

26

for $0 < y < 1$.

If we choose C_1 and C_2 in equation (45) as

$$
\begin{aligned}
C_1 &= \frac{1}{2} + \delta\pi(\tilde{H}(1) - \tilde{H}(0)) \\
C_2 &= \frac{1 - 2\ln(2)}{16} + \frac{\delta\pi}{2}(\tilde{H}(1) - \tilde{H}(0)) - \frac{\delta\pi\ln(2)}{2}(\tilde{H}(0) + \tilde{H}(1))
\end{aligned}
$$

then $\alpha(0) = \alpha(1) = 0$ and we find that ϕ is continuous on $[0, 1]$ with $\lim_{y \to 0+} \phi(y) = \lim_{y \to 1-} \phi(y) = 0$, and in fact

$$
\phi(y) = -\frac{1}{\pi}\sqrt{y - y^2} + \delta\psi_1(y) \tag{56}
$$

with

$$
\psi_1(y) = \frac{(\tilde{H}(0) - \tilde{H}(1))y - \tilde{H}(0) + \tilde{H}(y)}{\sqrt{y - y^2}} \tag{57}
$$

To verify the remaining properties of ϕ, let $r(y) = (\tilde{H}(0) - \tilde{H}(1))y - \tilde{H}(0) + \tilde{H}(y)$ so that $r(0) = 0$ and

$$
r'(y) = \tilde{H}(0) - \tilde{H}(1) + \tilde{H}'(y).
$$

From this and estimates (54), (55), we have

$$
r(y) = \int_0^y r'(x)\,dx \leq C\|f\|_{C^3}y.
$$

One can similarly obtain a bound $r(y) \leq C\|f\|_{C^3}(1-y)$, so that in fact $r(y) \leq C\|f\|_{C^3}(y-y^2)$ for $0 < y < 1$. Combining this with (57) provides a bound $\psi_1(y) \leq C\|f\|_{C^3}\sqrt{y - y^2}$, and in particular shows that ϕ is continuous on $[0, 1]$. Clearly $\|\psi_1\|_\infty \leq C\|f\|_{C^3}$. The estimate on $r(y)$ also make it simple to check that $\phi'(y)$ is integrable on $(0, 1)$ which completes the proof of the Lemma. $\square$.

Remark: A simple change of variables in the integral equation of the Lemma shows that the integral equation

$$
\text{p.v.} \int_0^\epsilon \frac{\phi'(t)}{t - s}\,dt = 1 + \delta f(s), \quad 0 < s < \epsilon, \tag{58}
$$

has a unique solution ϕ of the form

$$
\phi(t) = -\frac{1}{\pi}\sqrt{t(\epsilon - t)} + \delta\epsilon\psi_1(t)
$$

which is continuous on $[0, \epsilon]$, twice continuously-differentiable on $(0, \epsilon)$, with ϕ' integrable on $(0, \epsilon)$ and $\phi(0) = \phi(\epsilon) = 0$. Also, $\|\psi_1\|_\infty$ is bounded by $\|f\|_{C^3[0,\epsilon]}$.

27

5.3 The Main Theorem

Theorem 1 *Let σ_ϵ denote a linear crack with center $\mathbf{p}$, at angle θ, of length ϵ. Let u be the solution to the boundary value problem (1)-(3). Then*

$$\int_\sigma [u]\,ds = \frac{\pi}{4}(\nabla u_0(\mathbf{p}) \cdot \mathbf{n})\epsilon^2 + O(\epsilon^3).$$

Note that the $O(\epsilon^3)$ term may involve constant(s) that depend on $\mathbf{p}$ and/or θ. Throughout we will consider the midpoint $\mathbf{p}$ and angle θ fixed, but consider σ_ϵ as a function of ϵ; we will suppress this dependence and simply write σ when convenient.

Proof: After translation and rotation we may assume that $\mathbf{p}$ is the origin and the short crack σ_ϵ spans the interval $(0, \epsilon)$ along the x axis. Note that on the crack $\frac{\partial}{\partial \mathbf{n}} = \frac{\partial}{\partial y}$. Let d_0 denote the distance from σ_ϵ to $\partial\Omega$.

As discussed above, take v_0 to be defined by

$$v_0(x, y) = \int_0^\epsilon \frac{\partial G}{\partial y}(x - s, y)\phi(s)\,ds \qquad (59)$$

with ϕ chosen so that

$$\frac{\partial v_0}{\partial \mathbf{n}} = -\frac{\partial u_0}{\partial \mathbf{n}} \qquad (60)$$

and $\phi(0) = \phi(\epsilon) = 0$. As shown above we have, from Lemma 2 (and specifically, equation (58) and the following remarks) that ϕ is uniquely determined and is continuous on $[0, \epsilon]$, twice-continuously differentiable on $(0, \epsilon)$, with $\phi(0) = \phi(\epsilon) = 0$, of the form

$$\phi(s) = 2\frac{\partial u_0}{\partial y}(p, 0)\sqrt{s(\epsilon - s)} + \epsilon^2\psi_1(s) \qquad (61)$$

for some function ψ_1. Note that although ψ_1 depends on ϵ, $\|\psi_1\|_{L^\infty(0,1)}$ is bounded for ϵ in any neighborhood of zero (as is $\frac{\partial u_0}{\partial y}(p, 0)$).

Integrating over the crack shows that

$$\int_{\sigma_\epsilon} [v_0](s)\,ds = \frac{\pi}{4}\epsilon^2\frac{\partial u_0}{\partial y}(p, 0) + \epsilon^3\psi(\epsilon).$$

for some bounded function ψ. More generally, if σ_ϵ lies at an arbitrary angle with normal vector $\mathbf{n}$ we obtain

$$\int_{\sigma_\epsilon} [v_0](s)\,ds = \frac{\pi}{4}\epsilon^2\frac{\partial u_0}{\partial \mathbf{n}}(\mathbf{p}) + \epsilon^3\psi(\epsilon) \qquad (62)$$

where $\mathbf{p}$ denotes the midpoint of σ_ϵ (really, $\mathbf{p}$ can be any point along the crack).

28

Now from the definition of v_0 in equation (59) we have, for (x, y) away from σ_ϵ,

$$\frac{\partial v_0}{\partial x}(x, y) = \frac{1}{\pi} \int_0^\epsilon \frac{(x - s)y}{((x - s)^2 + y^2)^2} \phi(s)\, ds$$

$$\frac{\partial v_0}{\partial y}(x, y) = -\frac{1}{2\pi} \int_0^\epsilon \frac{(x - s)^2 - y^2}{((x - s)^2 + y^2)^2} \phi(s)\, ds$$

where without loss of generality we again assume that σ_ϵ coincides with the interval $(0, \epsilon)$ on the x axis. At any point on $\partial\Omega$ we can then bound

$$
\begin{aligned}
\left| \frac{\partial v_0}{\partial \mathbf{n}} \right| &= \left| n_1 \frac{\partial v_0}{\partial x} + n_2 \frac{\partial v_0}{\partial y} \right| \\
&\leq \sqrt{n_1^2 + n_2^2} \left(\left(\frac{\partial v_0}{\partial x} \right)^2 + \left(\frac{\partial v_0}{\partial y} \right)^2 \right)^{1/2} \\
&\leq \left(\frac{1}{4\pi^2} \int_0^\epsilon \frac{1}{((x - s)^2 + y^2)^2}\, ds \right)^{1/2} \left(\int_0^\epsilon \phi^2(s)\, ds \right)^{1/2} \\
&\leq C \frac{\sqrt{\epsilon}}{d_0^2} \sqrt{\epsilon^3 / 6} \\
&\leq \tilde{C} \epsilon^2
\end{aligned}
$$
(63)

for some constant $\tilde{C}$, where we have used $|\mathbf{n}| = 1$, the estimate (61), and recall that d_0 is the minimum distance from σ_ϵ to $\partial\Omega$.

Now let w_0 be the unique harmonic function on Ω with $\frac{\partial w_0}{\partial \mathbf{n}} = -\frac{\partial v_0}{\partial \mathbf{n}}$ on $\partial\Omega$ with normalization $\int_{\partial\Omega} w_0\, ds = 0$. Standard elliptic estimates show that $|\partial w_0 / \partial \mathbf{n}| \leq \tilde{C} \epsilon^2$ for some constant $\tilde{C}$ at all points on σ_ϵ.

Define a function $\tilde{u} = u_0 + v_0 + w_0$ on $\Omega \setminus \sigma_\epsilon$. Note that $\tilde{u}$ is harmonic, with $\frac{\partial \tilde{u}}{\partial \mathbf{n}} = g$ on $\partial\Omega$, $\int_{\partial\Omega} \tilde{u}\, ds = 0$, and

$$\frac{\partial \tilde{u}}{\partial \mathbf{n}} = \frac{\partial w_0}{\partial \mathbf{n}}$$
(64)

on σ_ϵ.

Claim: $\|\tilde{u} - u\|_{L^2(\partial\Omega)} \leq C \epsilon^3$ for some constant C which is independent of ϵ.

To prove the claim, we examine the function $r = u - \tilde{u}$. The function satisfies

$$
\begin{aligned}
\triangle r &= 0 \quad \text{in} \quad \Omega \setminus \sigma_\epsilon \\
\frac{\partial r}{\partial \mathbf{n}} &= 0 \quad \text{on} \quad \partial\Omega \\
\frac{\partial r}{\partial \mathbf{n}} &= -\frac{\partial w_0}{\partial \mathbf{n}} \quad \text{on} \quad \sigma_\epsilon
\end{aligned}
$$
(65)

29

with the normalization $\int_{\partial\Omega} r\, ds = 0$. Construct a function r_1 defined on $\Omega \setminus \sigma_\epsilon$ by

$$r_1(\mathbf{x}) = \int_{\sigma_\epsilon} \frac{\partial G}{\partial \mathbf{n}_y}(\mathbf{x} - \mathbf{s})\psi(\mathbf{s})\, ds \qquad (66)$$

analogous the definition of v_0 in equation (59), where ψ is a function to be specified. In fact, by Lemma 1 we can choose ψ so that r_1 satisfies $\frac{\partial r_1}{\partial \mathbf{n}} = \frac{\partial w_0}{\partial \mathbf{n}}$ on σ_ϵ. Moreover, since $|\frac{\partial w_0}{\partial \mathbf{n}}| \leq C_2 \epsilon^2$ at all point on σ_ϵ, we find that $|\psi|_{L^2 \sigma_\epsilon} \leq C_3 \epsilon^2$. Estimates analogous to those leading to (63) show that $|\frac{\partial r_1}{\partial \mathbf{n}}| \leq C_4 \epsilon^4$ on $\partial\Omega$, and it simple to estimate $|r_1| \leq C_5 \epsilon^3$ on $\partial\Omega$.

The function $r_2 = r + r_1$ is harmonic in $\Omega \setminus \sigma_\epsilon$ with $\frac{\partial r_2}{\partial \mathbf{n}} = \frac{\partial r_1}{\partial \mathbf{n}}$ on $\partial\Omega$ with

$$\frac{\partial r_2}{\partial \mathbf{n}} = 0$$

on σ_ϵ, and also $\int_{\partial\Omega} r_2\, ds = 0$. Integrating by parts shows that

$$\int_{\Omega \setminus \sigma_\epsilon} |\nabla r_2|^2\, dx = \int_{\partial\Omega} r_2 \frac{\partial r_1}{\partial n}\, ds. \qquad (67)$$

Thus

$$
\begin{aligned}
\|\nabla r_2\|_{L^2(\Omega \setminus \sigma_\epsilon)}^2 &\leq \|r_2\|_{L^2(\partial\Omega)} \|\frac{\partial r_1}{\partial n}\|_{L^2(\partial\Omega)} \\
&\leq C \|r_2\|_{H^1(\Omega \setminus \sigma_\epsilon)} \|\frac{\partial r_1}{\partial n}\|_{L^2(\partial\Omega)}
\end{aligned}
\qquad (68)
$$

in which the constant C can be made independent of σ, since σ_ϵ stays away from a neighborhood of $\partial\Omega$.

From standard elliptic theory we can bound

$$\|r_2\|_{L^2(\partial\Omega)} \leq C_6(\epsilon) \|\partial r_1 / \partial \mathbf{n}\|_{L^2(\partial\Omega)} \qquad (69)$$

where the constant C_6 may depend on ϵ. However, one can easily show that $C_6(\epsilon) < C_6(\epsilon_0)$ for $\epsilon < \epsilon_0$ where $\epsilon_0 > 0$ is fixed. Specifically, from $\triangle r_2 = 0$ in $\Omega \setminus \sigma_\epsilon$ with $\frac{\partial r_2}{\partial \mathbf{n}} = \frac{\partial r_1}{\partial \mathbf{n}}$ on $\partial\Omega$ and $\frac{\partial r_2}{\partial \mathbf{n}} = 0$ on σ_ϵ we obtain, from integration by parts,

$$\int_{\Omega \setminus \sigma_\epsilon} |\nabla r_2|^2\, dx = \int_{\partial\Omega} r_2 \frac{\partial r_1}{\partial \mathbf{n}}\, ds$$

so that

$$
\begin{aligned}
\|\nabla r_2\|_{L^2(\Omega \setminus \sigma_\epsilon)}^2 &\leq \|r_2\|_{L^2(\partial\Omega)} \|\partial r_1 / \partial \mathbf{n}\|_{L^2(\partial\Omega)} \\
&\leq C \|r_2\|_{H^1(\Omega \setminus \sigma_\epsilon)} \|\partial r_1 / \partial \mathbf{n}\|_{L^2(\partial\Omega)}
\end{aligned}
\qquad (70)
$$

30

for some constant C which can be taken independently of ϵ (provided σ_ϵ remains away from a fixed neighborhood of $\partial\Omega$; this may need filling out; consider neighborhood of $\partial\Omega$).

Now note that we can also obtain a bound

$$\|r_2\|_{L^2(\Omega\setminus\sigma_\epsilon)} \leq C\|\nabla r_2\|_{L^2(\Omega\setminus\sigma_\epsilon)} \tag{71}$$

where C is independent of ϵ. To see this, note that the smallest eigenvalue for the Laplacian on the space $V(\epsilon) = \{\phi \in H^1(\Omega \setminus \sigma_\epsilon), \int_{\partial\Omega} \phi \, ds = 0\}$ is given by

$$\lambda_\epsilon = \inf_{V(\epsilon)} \frac{\|\nabla\phi\|_{L^2(\Omega\setminus\sigma_\epsilon)}}{\|\phi\|_{L^2(\Omega\setminus\sigma_\epsilon)}} = \inf_{V(\epsilon)} \frac{\|\nabla\phi\|_{L^2(\Omega)}}{\|\phi\|_{L^2(\Omega)}}$$

where we extend by zero to all of Ω. Since $V(\epsilon_1) \subset V(\epsilon_2)$ for $\epsilon_1 < \epsilon_2$, we clearly have $\lambda_{\epsilon_1} \geq \lambda_{\epsilon_2}$ for $\epsilon_1 < \epsilon_2$. Fix $\epsilon_0 > 0$ so that for all $\epsilon < \epsilon_0$ we have $\lambda_\epsilon \geq \lambda_{\epsilon_0}$. It then follows that for $\phi \in V(\epsilon)$ we have

$$\frac{\|\nabla\phi\|_{L^2(\Omega\setminus\sigma_\epsilon)}}{\|\phi\|_{L^2(\Omega\setminus\sigma_\epsilon)}} \geq \lambda_\epsilon \geq \lambda_{\epsilon_0}.$$

A bit of rearrangement gives

$$\|\phi\|_{L^2(\Omega\setminus\sigma_\epsilon)} \leq \frac{1}{\lambda_{\epsilon_0}}\|\nabla\phi\|_{L^2(\Omega\setminus\sigma_\epsilon)}$$

which shows inequality (71).

From (71) we immediately obtain

$$\|r_2\|_{H^1(\Omega\setminus\sigma_\epsilon)} \leq \|r_2\|_{L^2(\Omega\setminus\sigma_\epsilon)} + \|\nabla r_2\|_{L^2(\Omega\setminus\sigma_\epsilon)} \leq C\|\nabla r_2\|_{L^2(\Omega\setminus\sigma_\epsilon)}. \tag{72}$$

Combining inequalities (70) and (72) shows that

$$\|r_2\|_{H^1(\Omega\setminus\sigma_\epsilon)} \leq C\|\partial r_1/\partial\mathbf{n}\|_{L^2(\partial\Omega)}$$

for some constant C which is independent of ϵ. From this we obtain the estimate (69) with C independent of ϵ.

As a consequence of (69) we find that $\|r_2\|_{L^2(\partial\Omega)} = O(\epsilon^4)$. It follows that $\|u - \tilde{u}\|_{L^2(\partial\Omega)} = \|r\|_{L^2(\partial\Omega)} = \|r_1 - r_2\|_{L^2(\partial\Omega)} = O(\epsilon^3)$, as the Claim asserts.

With the Claim established, we now note that

$$\int_\sigma [u]\, ds = \int_\sigma [\tilde{u}]\, ds + \int_\sigma [r]\, ds.$$

31

But since $\int_\sigma [r]\, ds$ can be computed as $\int_{\partial\Omega} r\psi\, ds$ for a suitable function ψ (independent of the crack length ϵ) we conclude that $\int_\sigma [r]\, ds = O(\epsilon^3)$ and so

$$\int_\sigma [u]\, ds = \int_\sigma [\tilde{u}]\, ds + O(\epsilon^3).$$

But $[\tilde{u}] = [u_0] + [v_0] + [w_0] = [v_0]$. As a result

$$\int_\sigma [\tilde{u}]\, ds = \int_\sigma [v_0]\, ds$$

and from equation (62) we obtain

$$\int_\sigma [u]\, ds = \frac{\pi}{4}\epsilon^2 \frac{\partial u_0}{\partial \mathbf{n}}(\mathbf{p}) + O(\epsilon^3)$$

which proves Theorem 1.

6 Conclusion

In this paper, we offered an alternative algorithm for accurately locating a single, perfectly insulating, linear crack in a two dimensional region. This algorithm relied on concepts from linear algebra and, more importantly, analysis leading to the relation of the crack length to the integral of the temperature jump over the crack. We then employed the ideas from this algorithm in the numerical approximation of the locations of multiple small, perfectly insulating, linear cracks. This numerical approximation is improved from other methods inasmuch as it does not rely on solving a boundary value problem. Removing this necessity greatly expedites the process of locating multiple cracks. We also proved that an optimal heat influx, g, always exists, and can be found explicitly for any two-dimensional region. Finally, we included a example of the algorithm used in the location of a single crack in the region of the unit disk and several examples of the numerical approximation of the locations of multiple cracks inside of the unit disk.

There are many unexplored facets to this problem. First, as demonstrated in the Crack Reconstruction Section, it is important to know the number of cracks lying in a region before attempting to approximate their locations. Does the α function give some sort of indication about the number of cracks lying inside of a particular region? Does there exist some method by which the number of cracks can be ascertained before attempting numerical reconstruction?

Also, could the algorithm offered for locating a single crack be extended to cracks which are non-linear in some fashion? Would it offer any indication about the shape of the crack? However, due to the fact that our approximation basically treated the entire crack as being

the midpoint, some work would have to be done with $\frac{\partial \Gamma}{\partial \mathbf{n}}$ without employing this approximation, perhaps using integration by parts.

The most interesting problem, however, is to rid the necessity of using approximate numerical methods to locate multiple cracks. The trouble here is determining which characteristics of (5) are influenced by which crack. Essentially, we need to find the individual constituents of a sum given only the sum. Is there some way in which the approximation employed in locating a single crack can be generalized to multiple cracks without relying on purely numerical methods?

References

[1] Andersen, K., Brooks, S., and Hansen, M., *A Bayesian approach to crack detection in electrically conducting media*, Inverse Probl, **17**, 2001, pp. 121-136.

[2] Bryan, K., Vogelius, M., A uniqueness result concerning the identification of a collection of cracks from finitely many electrostatic boundary measurements, Siam J. Math. 6, 1992, pp 950-958.

[3] Alessandrini, F., and Diaz Valenzuela, A., Unique determination of multiple cracks by two measurements, Siam J Cont Opt, 34 (3), 1996, pp. 913-921.

[4] Andrieux, S., Ben Abda, A., and Bui, H.D., Reciprocity principle and crack identification, Inverse Probl, 15 (1), 1999, pp. 59-65.

[5] Ogborne, F., and Vellela, M., Reconstruction of Cracks with Unknown Transmission Condition from Boundary Data, Rose-Hulman Mathematical Technical Report, Summer 2002.

[6] Bryan, K., Vogelius, M., Reconstruction of multiple cracks from experimental electrostat-icboundary measurements, Inverse Problems and Optimal Design in Industry, 7, 1993, pp. 147-167.

[7] Porter, D. and Stirling, D., Integral Equations: a pracitcal treatment, from spectral theory to applications.